Mathematical modeling and kinematic analysis of 5 degrees of freedom serial link manipulator for online real-time pick and place applications

Abhilasha Singh[1], Kalaichelvi Venkatesan[1], Yuvalakshmi Nagarasan[1], Karthikeyan Ramanujam[2], Kumar Karuppusamy[3]

[1]Department of Electrical and Electronics Engineering, Birla Institute of Technology and Science Pilani, Dubai Campus UAE, Dubai, United Arab Emirates
[2]Department of Mechanical Engineering, Birla Institute of Technology and Science Pilani, Dubai Campus UAE, Dubai, United Arab Emirates
[3]Department of Mathematics, Birla Institute of Technology and Science Pilani, Dubai Campus UAE, Dubai, United Arab Emirates

Article Info	ABSTRACT
	Modeling and kinematic analysis are crucial jobs in robotics that entail identifying the position of the robot's joints in order to accomplish particular tasks. This article uses an algebraic approach to model the kinematics of a serial link, 5 degrees of freedom (DOF) manipulator. The analytical method is compared to an optimization strategy known as sequential least squares programming (SLSQP). Using an Intel RealSense 3D camera, the colored object is picked up and placed using vision-based technology, and the pixel location of the object is translated into robot coordinates. The LOBOT LX15D serial bus servo controller was used to transmit these coordinates to the robotic arm. Python3 programming language was used throughout the entire analysis. The findings demonstrated that both analytical and optimized inverse kinematic solutions correctly identified colored objects and positioned them in their appropriate goal points. *This is an open access article under the <u>CC BY-SA</u> license.*

Corresponding Author:

Abhilasha Singh
Department of Electrical and Electronics Engineering, Birla Institute of Technology and Science Pilani
P.O. Box 345 055, Dubai Campus, Dubai, United Arab Emirates
Email: p20180906@dubai.bits-pilani.ac.in

1. INTRODUCTION

Robots play a significant role in industrial automation, where they employ machine vision to recognize and categorize the objects put so they can pick and place them quickly [1]. Vision sensors are employed to collect visual feedback data on the scattered objects in the surroundings for this task. The efficient picking of things by the robot requires an understanding of dynamics and kinematics [2]. Robot dynamics deals with joint force and torque, whereas kinematic analysis determines the position of the robot joints without taking force into account [3]. The kinematics and inverse kinematics of a 5 degrees of freedom (DOF) robotic arm are covered in this work. One of the most significant tasks involves selecting the ideal robot from the available conventional configurations. This requires designing the working positions required for forward and inverse kinematics modeling [4]. The joint angles are used to determine the position of the end effector in forward kinematics, whereas the end effector position is used to determine the joint angles in inverse kinematics. The two methods of inverse kinematics algorithms are closed-form solutions and numerical approaches [5]. The closed-form solutions are found using algebraic and geometric techniques, and the Jacobian transpose method [6], pseudoinverse method [7], cyclic coordinate descent methods [8],

optimization algorithms [9], artificial intelligence (AI) methods [10], and singular value decomposition [11] are some of the widely utilized numerical techniques. Since closed-form solutions require precise initial values and converge more quickly than numerical ones, an algebraic approach was taken in this study to calculate joint angles. Gaeid *et al.* [3] used Denavit-Hartenberg (DH) parameters and matrix transformation method to perform kinematic modeling of 6 DOF manipulator whereas Sutyasadi and Wicaksono [12] used hybrid controller of iterative learning and H∞ controller to control the robot joint for trajectory tracking applications. Quang *et al.* [13] used radial basis function to derive the inverse dynamics of delta manipulator and Mashhadany [14] used adaptive neuro fuzzy inference system (ANFIS) controller and fractional order proportional, integral, derivative (FOPID) controller to obtain optimal trajectory for PUMA 560 manipulator. Dewi *et al.* [15] implemented fruit sorting robot for packaging industry using hue saturation value (HSV) and image processing techniques. In the above discussed works kinematic analysis has been implemented in servo motors with conventional controllers. Also, most of the works were tested on simulation. Hence in this paper the main contribution of this work is to implement vision-based control for pick and place operation for different colors and object size. To obtain joint commands, inverse kinematics solutions for Lewansoul xArm manipulator made up of serial bus servo motors is derived. The main difference between serial bus servo and other servo motors is that serial bus servo motors are connected serially. In such motors, when one motor does not receive power, the other motors does not work. Secondly, attempt has been made to perform real time experimentation for industrial pick and place operation from live IntelRealSense camera feed. This work can be commonly used in color-based objects sorting, garbage sorting and picking up the fruits based on their color, size, and shape.

2. PROPOSED METHOD

The method suggested in this study involves taking screenshots of each frame taken by the Intel RealSense camera and using HSV morphology and HSV transformation to extract the features of the colored objects. To acquire the specific channel needed to draw the contours around the objects, the colors are further masked. Then, camera-to-robot coordinates (x, y, z) are determined via homogeneous transformation. Inverse kinematics solutions utilizing the algebraic approach and sequential least squares programming (SLSQP) are compared using these coordinates. By positioning the Intel RealSense camera in an eye-to-hand position, the joint angles that were obtained are used to implement pick and place operations. Finally, these robot joint commands are transferred to the Lewansoul xArm robotic arm to conduct pick and place of the relevant colored objects [16]. The xArm-SDK was used throughout the entire procedure and during real-time experimentation in the Python3 environment. Figure 1 depicts the overall process flow for a vision-based pick and place operation.
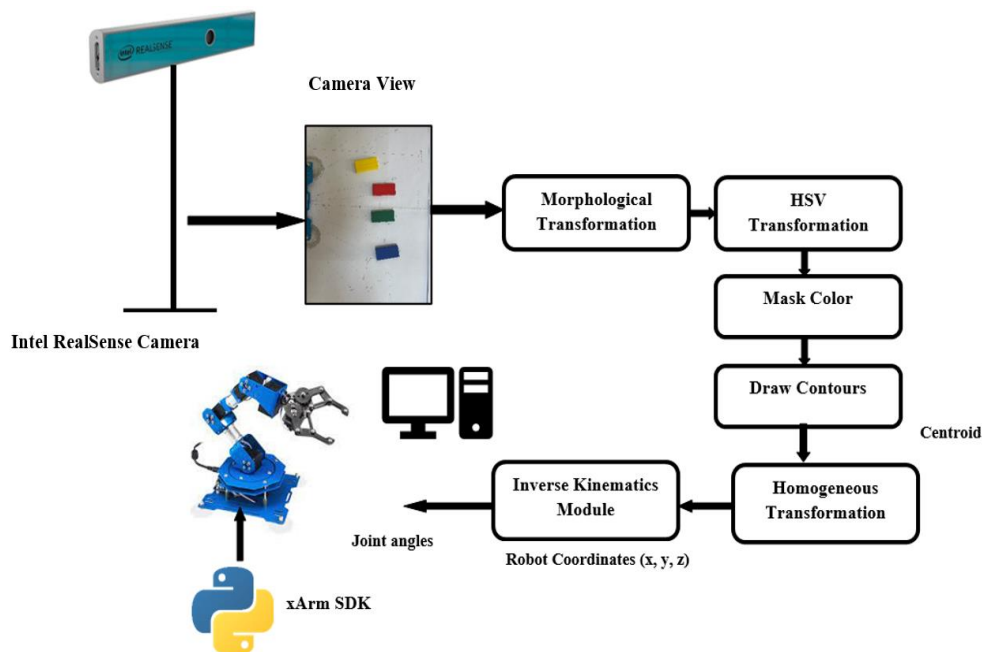

Figure 1. Process flow of vision-based pick and place using Lewansoul xArm manipulator

3. METHOD

3.1. Kinematic modelling of Lewansoul xArm

In this section, detailed modelling of kinematics and inverse kinematics is discussed for Lewansoul xArm which is a 5 DOF robotic arm which is used for gripping, sorting, and many other industrial applications. It is a miniature version of an industrial manipulator that runs with intelligent bus servos LX-15D servo motor which has built-in position feedback and voltage feedback. The xArm is controlled by using wireless handle control and through smartphone app [17]. This arm can be operated in robot operating system (ROS) and Python 3, but the entire work reported in this paper is carried out in python 3.6. The python wrapper called xArm is installed which has built-in functions to operate the robot. In this paper, DH method is used which is used for finding the transformation matrix between each joint. Initially, robot links length and angles between joints are measured and tabulated for xArm. Next, each row in the DH table corresponds to transformation between each joint. Finally, the overall transformation matrix is obtained between the end effector to the base of the robot [18]. The basic parameters obtained are θ_i=angle from x_{i-1} to x_i along z_{i-1}; d_i=distance from the intersection of z_{i-1} with x_i to the origin of $(i-1)$ system of axes; a_i=distance between z_{i-1} and z_i; α_i =angle from z_{i-1} to z_i along x_i.

3.1.1. Forward kinematics of Lewansoul xArm

The forward kinematics involves finding the position of the robot end-effector with joint angles as inputs [19]. The kinematic diagram of Lewansoul 5 DOF robotic manipulator with individual joint axes is shown in Figure 2 where Figure 2(a) represents the frame mapping of individual joints and Figure 2(b) represents the RoboAnalyser model of manipulator which is efficient tool for analyzing the frames. Using the link length and link biases measurements from the Figure 2, the DH parameters for 5 DOF manipulator is shown in Table 1. Since the gripper is the 6th joint, it is not included in the DH parameter calculation.

Table 1. DH parameters of Lewansoul xArm robotic manipulator

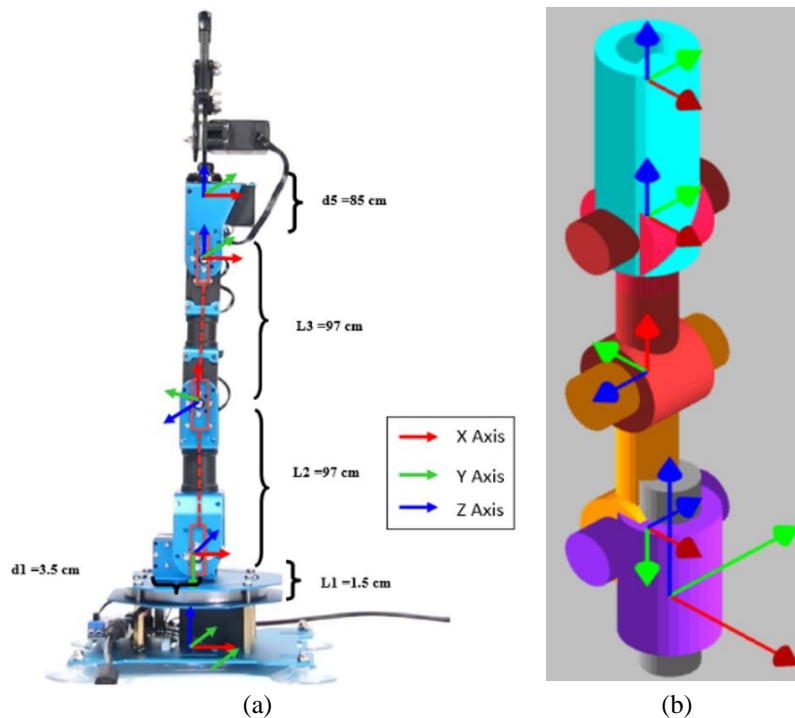| a	α	d	θ
-0.015	-90	0.035	θ_1
0.097	180	0	$\theta_2 - 90$
0.097	180	0	θ_3
0	90	0	$\theta_4 + 90$
0	0	0.085	θ_5

Figure 2. Kinematic scheme of Lewansoul xArm manipulator (a) frames of each joints and (b) visualization of frames in RoboAnalyser

The individual transformation matrices of joints are formulated using (1) [14],

$$^{i-1}_iT = \begin{bmatrix} C\theta & -S\theta C\alpha & S\theta S\alpha & aC\theta \\ S\theta & C\theta C\alpha & -C\theta S\alpha & aS\theta \\ 0 & S\alpha & C\alpha & d \\ 0 & 0 & 0 & 1 \end{bmatrix} \tag{1}$$

where i=no. of frames varying from 0 to 4 for xArm; $\cos(x) = Cx$; $\sin(x) = Sx$ $x=\theta$ or α. The overall transformation matrix ^5_0T from the end effector to the base of the robot is obtained.

$$^5_0T = {}^5_4T \times {}^4_3T \times {}^3_2T \times {}^2_1T \times {}^1_0T \tag{2}$$

$$^5_0T = \begin{bmatrix} -1 & 0 & 1 & -0.015 \\ 0 & 1 & 0 & 0 \\ 0 & 0 & -1 & 0.314 \\ 0 & 0 & 0 & 1 \end{bmatrix} \tag{3}$$

From (3), the first three rows and columns denote the initial rotation matrices R, and the last column denotes the initial position of the end effector. Therefore, the home position of the xArm manipulator is (-15,0,314) mm respectively.

3.1.2. Inverse kinematics of Lewansoul xArm

The inverse kinematics involves finding the individual joint angles of the robot arm using the position information in cartesian space. In this paper, inverse kinematics of xArm is derived using algebraic method and it is compared with optimization approach called SLSQP [20]. The analytical approach gives robust solutions since it involves trigonometric relationships and algebraic equations that determine the behavior of the degrees of freedom in the manipulator [21]–[23]. Here for simplicity, wrist angles are made zero and θ02-34 wrist angle relative to ground (WARTG) is taken as a constant value [24]. To start with, the overall transformation matrix from the end effector to base ^0_5T is obtained from equations from (3) and is taken as (4).

$$^5_0T = T_E = \begin{bmatrix} n_x & o_x & a_x & p_x \\ n_y & o_y & a_y & p_y \\ n_z & o_z & a_z & p_z \\ 0 & 0 & 0 & 1 \end{bmatrix} \tag{4}$$

Take (5).

$$A_1 = {}^0_1T; \ A_2 = {}^1_2T; \ A_3 = {}^2_3T; \ A_4 = {}^3_4T; \ A_5 = {}^4_5T \tag{5}$$

Consider (6).

$$A_2A_3A_4A_5 = A_1^{-1} \begin{bmatrix} n_x & o_x & a_x & p_x \\ n_y & o_y & a_y & p_y \\ n_z & o_z & a_z & p_z \\ 0 & 0 & 0 & 1 \end{bmatrix} \tag{6}$$

Solving LHS of the (6) we get (7).

$$\begin{bmatrix} C_1n_x + S_1n_y & C_1o_x + S_1o_y & C_1a_x + S_1a_y & C_1p_x + S_1p_y \\ -n_z & -o_y & -a_y & -p_z + d_1 \\ -S_1n_x + C_1n_y & -S_1o_x + C_1o_y & -S_1a_x + C_1a_y & -S_1p_x + C_1p_y \\ 0 & 0 & 0 & 1 \end{bmatrix} \tag{7}$$

Solving RHS of the (6) we get (8):

$$\begin{bmatrix} C_{2-34}C_5 & -C_{2-34}S_5 & -S_{2-34} & -S_{2-34}d_5 + a_3C_{23} + a_2C_2 \\ S_{2-34}C_5 & -S_{2-34}S_5 & C_{2-34} & -C_{2-34}d_5 - a_3S_{23} - a_2S_2 \\ S_5 & C_5 & 1 & 0 \\ 0 & 0 & 0 & 1 \end{bmatrix} \tag{8}$$

where θ_{2-34} is taken as $\theta_2 - \theta_3 + \theta_4$. By comparing (7) and (8) we get the values of joint angles which is,

$$\theta_1 = tan^{-1}\left(\frac{p_y}{p_x}\right) \tag{9}$$

where (p_x, p_y) is the end-effector position of the robot. Assuming WART configuration $\theta_{234} = 0$ to obtain θ_3.

$$\theta_3 = tan^{-1}\left(\frac{S_3}{C_3}\right) \tag{10}$$

Finally,

$$\theta_2 = tan^{-1}\left(\frac{S_2}{C_2}\right) \tag{11}$$

$$\theta_5 = tan^{-1}\left(\frac{S_5}{C_5}\right) \tag{12}$$

$$\theta_4 = \theta_{2-34} - \theta_2 + \theta_3 \tag{13}$$

The results obtained from algebraic method is compared with SLSQP which is an iterative method for constrained nonlinear optimization problem. This algorithm transforms the least squares model into the quadratic optimization model and the optimal solution can then be obtained by sequential quadratic programming. The nonlinear programming is of the form (14).

$$\min_x f(x) \tag{14}$$

Subject to $b(x) \geq 0; c(x) = 0$. Then at every iteration x_k quadratic programming sub problem is given by (15).

$$\min_d f(x) + \nabla f(x_k)^T d + \frac{1}{2} d^T \nabla^2 f(x_k)d \tag{15}$$

Subject to $b(x_k) + \nabla b(x_k)^T d \geq 0 \; ; c(x_k) + \nabla c(x_k)^T d = 0$.

3.2. Vision-based pick and place operation

In this section, inverse kinematics solutions obtained are used for pick and place operation. In general, pick and place using vision systems is common in almost all industries, but it still lags accuracy and efficiency. Hence there is the need to improve the process of picking up objects, possibly using intelligent techniques [25]. In recent times, there are many works, and improvements made in computer vision applications. In this paperwork, detailed steps of kinematic design and its application to pick and place using a 3D camera are discussed and also tested in real-time. This work gives the reader a clear idea about the mathematics behind the robotic arm and also how to implement computer vision tasks in real-time. The process flow for color extraction is shown in Figure 3.

Initially, the colored objects are placed in the robot workspace and the frames are captured by Intel RealSense camera attached to the wooden frame. The camera is placed in eye-to-hand configuration at an angle of 90° facing the objects [26]. Once the frames are captured HSV conversion takes place to extract the color of the objects. In this paper, four colors are used-red, green, blue, and yellow. The upper and lower range of HSV hue range of these colors were specified to mask each color and perform image dilation. Next contours are created around each color and its bounding box coordinates are extracted along with box coordinates to find the orientation of the shape. Another main contribution of this work is that without using a grasping dataset or training deep learning model, a simple and robust solution to find the grasping angle is implemented in this work. Using the adjacent box coordinates (x_1, y_1) and (x_2, y_2), the angle of rotation is found by measuring the length of both opposite sides and adjacent sides [27]. The centroid (C_x, C_y) of the bounding boxes is also obtained which is useful for the robot to understand the position of the object.

The formula for calculating the orientation is given by (16).

$$\theta = tan^{-1}\left(\frac{length\ of\ opp\ side}{length\ of\ adjacent\ side}\right) = tan^{-1}\left(\frac{y_2 - y_1}{x_2 - x_1}\right) degrees \tag{16}$$

Using all the above pixel information, T_b^c the transformation between camera frame $\{c\}$ and robot base $\{b\}$ is obtained using the homogeneous transformation technique which converts pixel to world coordinates so that robot can understand the points [28] as shown in Figure 4. Figure 4(a) illustrates the transformation between camera and robot base whereas Figure 4(b) explains the calculation of bounding box coordinates in xy plane.
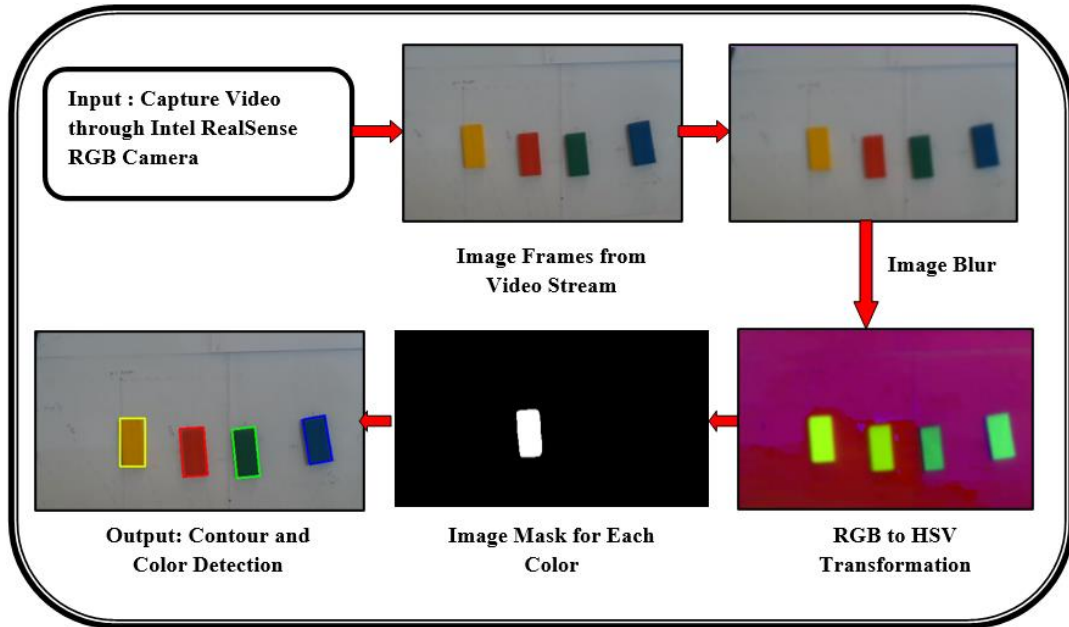

Figure 3. Process flow of color extraction using image processing for pick and place operation

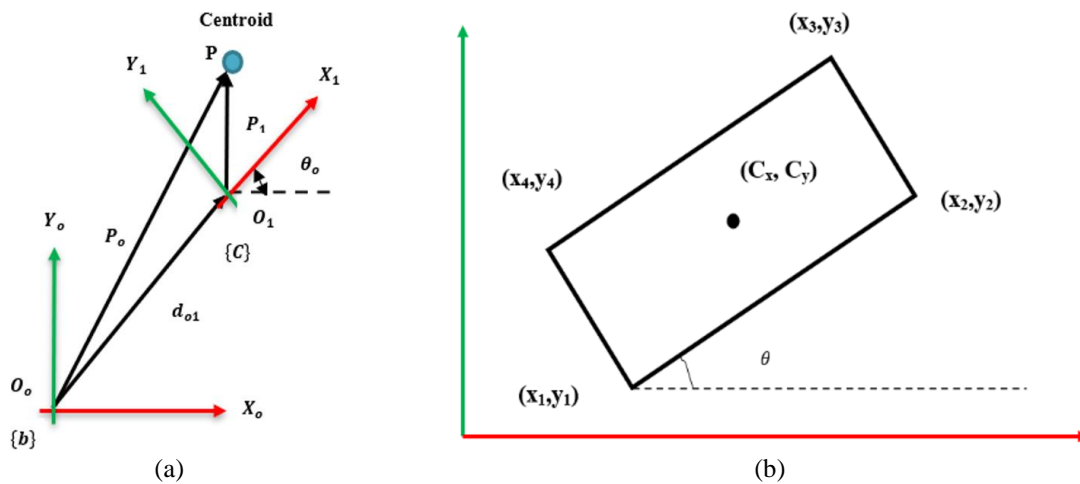(a)   (b)

Figure 4. Homogeneous coordinate transformation (a) transformation of centroid pixel point P from camera frame to robot base frame and (b) schematic diagram of bounding box for finding the orientation

The general equation for transforming a point from one frame to another frame is,

$$\begin{bmatrix} P^c \\ 1 \end{bmatrix} = \begin{bmatrix} R_c^b + d_0^1 \\ 1 \end{bmatrix} = \begin{bmatrix} R_c^b & d_c^b \\ 0^T & 1 \end{bmatrix} \begin{bmatrix} P \\ 1 \end{bmatrix} \tag{17}$$

In general,

$$P_0 = T_c^b \, P \; and \; T_c^b = P_0 P^{-1} \tag{18}$$

where P_0 is 4xm robot coordinates with respect to the robot base; P is 4xn camera coordinates with respect to world coordinates; T_c^b is 4x4 transformation matrix between camera and robot base; R_c^b is a 4×4 rotation matrix between camera and robot base.

In this work for the formation of P^c matrix, the pixel values of the robot workspace are obtained so that the entire workspace can be mapped globally. Here the centroid is the input which is converted to robot coordinates (x, y, z). Finally, these cartesian coordinates are converted into joint angles θ_1 to θ_5 for picking the object. If the pieces are oriented, the angle is fed directly to the wrist so that it orients itself similar to the object placed.

4.   RESULTS AND DISCUSSION

In this section results obtained from the algebraic and optimization approach are used for performing pick and place in real-time. The camera captures the colored object kept in the robot workspace using OpenCV. Once the color is detected it draws corresponding contours over the objects and its centroid is found out. The 2D workspace bounds of xArm are 50 to 300 mm in x direction (vertical) and -270 to +270 mm in y direction (horizontal) with -120 to +120 degree as joint limits for all the 5 joints. The 2D workspace plot for xArm is shown in Figure 5. Figure 5(a) shows the reachable area of robot in MATLAB whereas Figure 5(b). shows the real time workspace setup. The 3D workspace of the robot analyzed in RoboAnalyser is shown in Figure 5(c). From the figure, it can be inferred that this robot has spherical workspace until it reaches 435 mm. The real-time experimentation of picking colored objects is shown in Figure 6 where Figure 6(a) shows the experimental setup with Intel RealSense camera whereas Figures 6(b)-(c) show the live detection of colored objects using the input from the camera feed. The bounding boxes is drawn around the identified objects and the centroid and angle of rotation is calculated using the (16). These pixels are transformed into real world coordinates and finally inverse kinematics is used to find the joint angles for picking the specific objects in its workspace.
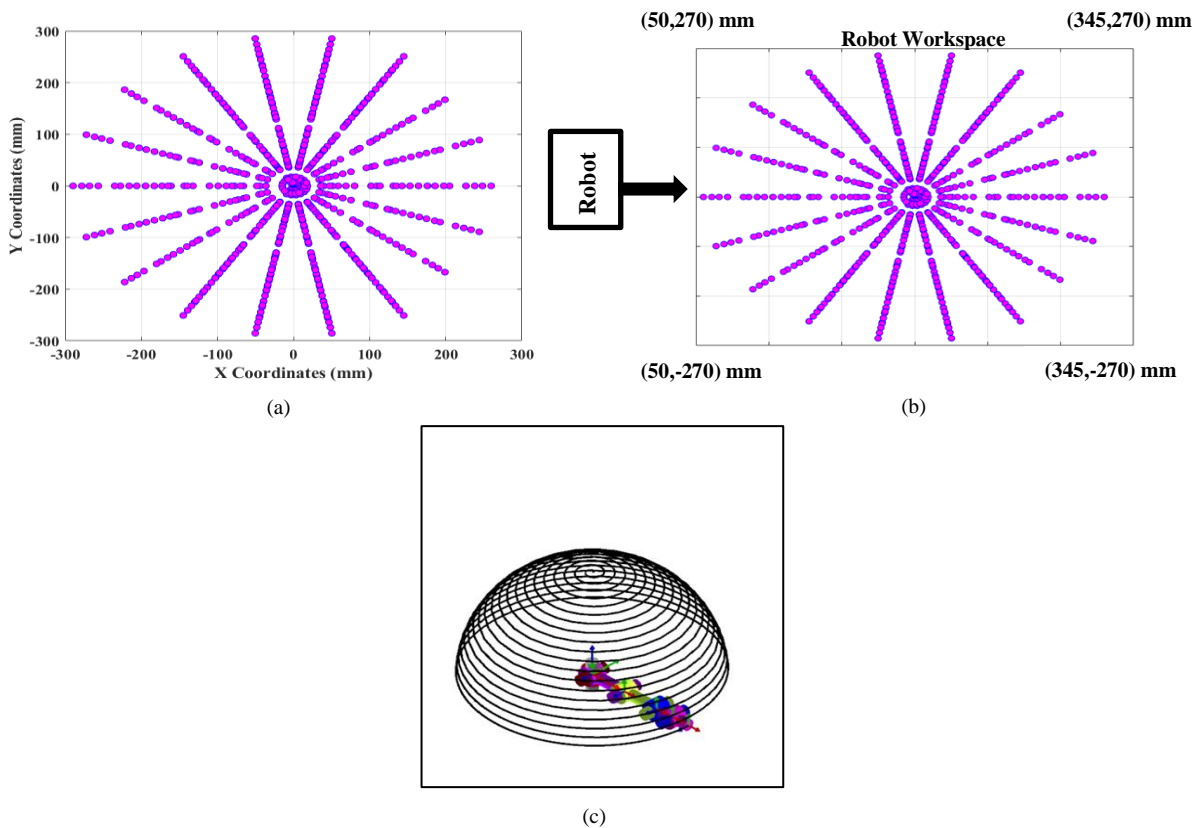

Figure 5. Illustration of xArm workspace (a) 2D workspace of manipulator (b) real-time experimental workspace (c) 3D workspace in RoboAnalyser
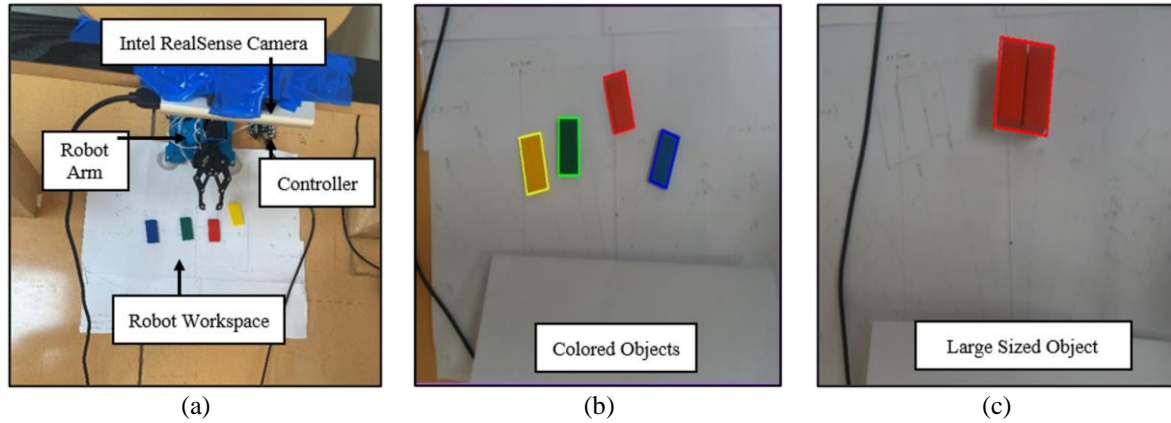
(a)   (b)   (c)

Figure 6. Experimental analysis (a) real-time vision-based pick, place (b) live detection of different size, and (c) colored objects using Intel RealSense camera

The HSV hue ranges of different colors, the orientation of the objects, and centroid are listed in Table 2. The hue ranges can be adjusted according to the resolution of the camera. These centroids obtained are in pixels which are further converted to robot coordinates (x, y, z) using a homogeneous transformation matrix as shown below. The robot coordinates are further converted into joint angles and sent to the robot for picking the object. The coordinates for placing the objects in the workspace were kept constant and it is chosen as $(200, -150)$ mm. The joint angles for pick and place obtained from the inverse kinematics algorithm for the yellow-colored object found are listed in Table 3.

$$\text{T} = \begin{bmatrix} 0 & -0.6145 & 0 & 345 \\ 0.843 & 0 & 0 & -270 \\ 0 & 0 & 0 & 0 \\ 0 & 0 & 0 & 1 \end{bmatrix} \tag{19}$$

Table 2. Experimental parameters of Lewansoul xArm robotic manipulator

Color	HSV range (Upper)	HSV range (Lower)	Centroid	Angle(degrees)
Yellow	(30,255,255)	(54,255,255)	(212,232)	14.47
Red	(10,255,255)	(0,100,20)	(275,180)	6.00
Green	(86,255,255)	(36,25,25)	(354,179)	10.12
Blue	(150,255,255)	(100,150,0)	(453,160)	8.74

Table 3. Comparative analysis of optimal inverse kinematics solutions using analytical method and SLSQP

Color	Centroid (Pixels)	Transformed Coordinates (mm)	SLSQP	Algebraic
Yellow	(212,232)	(202.41,-91.125,0)	$\theta_1=24.23$	$\theta_1=23.56$
			$\theta_2=65.82$	$\theta_2=64.32$
			$\theta_3=-19.80$	$\theta_3=-19$
			$\theta_4=79.53$	$\theta_4=80.5$
			$\theta_5=0$	$\theta_5=0$
Red	(359,89)	(289.99,-33.75,0)	$\theta_1=-2.53$	$\theta_1=-2.03$
			$\theta_2=78.096$	$\theta_2=77$
			$\theta_3=19.22$	$\theta_3=19.53$
			$\theta_4=67.09$	$\theta_4=67.5$
			$\theta_5=0$	$\theta_5=0$
Green	(188,102)	(282.31,-111.37,0)	$\theta_1=-22.31$	$\theta_1=-22.43$
			$\theta_2=63.35$	$\theta_2=63$
			$\theta_3=-9.23$	$\theta_3=-9.22$
			$\theta_4=65.29$	$\theta_4=65.34$
			$\theta_5=0$	$\theta_5=0$
Blue	(504,93)	(287.84,-156.37,0)	$\theta_1=-28.52$	$\theta_1=-28.65$
			$\theta_2=76.56$	$\theta_2=76.4$
			$\theta_3=-1.985$	$\theta_3=-1.98$
			$\theta_4=43.42$	$\theta_4=43.44$
			$\theta_5=0$	$\theta_5=0$

From the Table 3, it can be seen that the centroid of all the colored objects in pixels was converted into robot coordinates using the (31). Further, these coordinates were converted into joint angles and these angles were sent to the robot and tested the pick and place in real-time. The gripper angle was kept constant of about 30° as it was found to be effective for holding the objects. The robot was able to pick the objects and place them in the proper goal points efficiently. The same was tested with other colored blocks. The experimental parameters are illustrated in Figure 7. The joint angles obtained from SLSQP for blue object with time period of 1,000 ms is shown in Figure 7(a) and triangular angular velocity profile is illustrated in Figure 7(b). The real-time experimentation of vision-based pick and place was tested and is illustrated in Figure 8. The real-time experimentation of vision-based pick and place was tested with initial grasping position as shown in Figure 8(a). The picking of the red object is illustrated in Figure 8(b) whereas the red object reaching final point is shown in Figure 8(c).
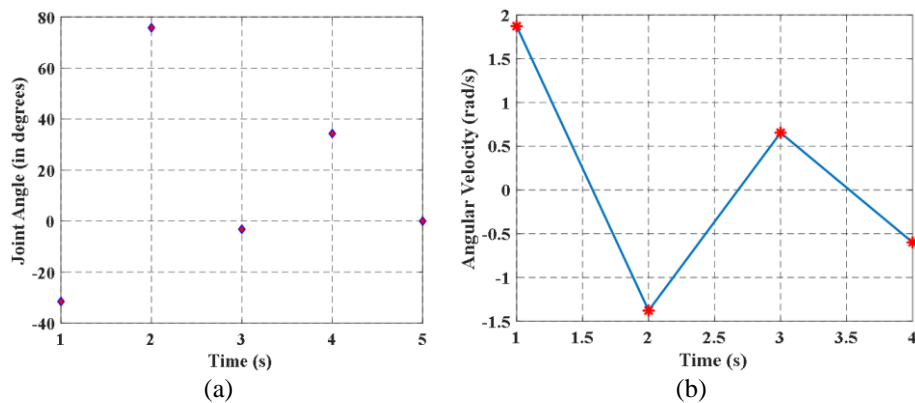

Figure 7. Graphical illustration of xArm parameters (a) joint angles for blue object and
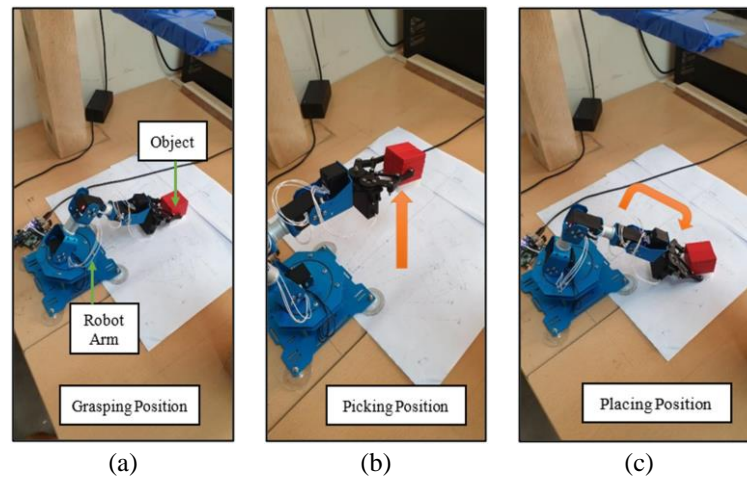(b) angular velocity of xArm

Figure 8. Real-time pick and place of colored objects (a) pick position (b) middle position,
and (c) place position

5.   CONCLUSION

Using the 3D camera in real-time, the online experimentation of vision-based pick and place operation was accomplished. This method can be used in industries to separate or identify the items placed on a conveyor belt. In agriculture and warehouse applications, they can be used to color-sort vegetables or other items. Under this article, colorful objects could be reliably identified even in a variety of illumination and noise situations. The algebraic technique was used to mathematically derive the inverse kinematics. It was discovered that the algebraic technique and the SLSQP optimization method both produced effective solutions with only a slight difference in error. In almost every location in the workspace, the coordinate

conversions were exact and correctly positioned the objects. During the real-time experimentation, these minor errors had very little effect. A more realistic experimental setup for identifying industrial objects that match the industrial environment will be included in future developments. Deep learning approaches can be used in conjunction with additional inverse kinematics methods to detect the objects.

REFERENCES

[1]   M. Javaid, A. Haleem, R. P. Singh, S. Rab, and R. Suman, "Exploring impact and features of machine vision for progressive industry 4.0 culture," *Sensors International*, vol. 3, 2022, doi: 10.1016/j.sintl.2021.100132.

[2]   K. Renuka, N. Bhuvanesh, and J. R. Catherine, "Kinematic and dynamic modelling and PID control of three degree-of-freedom robotic arm," in *Springer Proceedings in Materials*, Springer Singapore, 2021, pp. 867–882.

[3]   K. S. Gaeid, A. F. Nashee, I. A. Ahmed, and M. H. Dekheel, "Robot control and kinematic analysis with 6DoF manipulator using direct kinematic method," *Bulletin of Electrical Engineering and Informatics (BEEI)*, vol. 10, no. 1, pp. 70–78, Feb. 2021, doi: 10.11591/eei.v10i1.2482.

[4]   J. Cai, J. Deng, W. Zhang, and W. Zhao, "Modeling method of autonomous robot manipulator based on D-H algorithm," *Mobile Information Systems*, pp. 1–10, Jul. 2021, doi: 10.1155/2021/4448648.

[5]   R. Singh, V. Kukshal, and V. S. Yadav, "A review on forward and inverse kinematics of classical serial manipulators," in *Lecture Notes in Mechanical Engineering*, Springer Singapore, 2021, pp. 417–428.

[6]   S.-O. Park, M. C. Lee, and J. Kim, "Trajectory planning with collision avoidance for redundant robots using Jacobian and artificial potential field-based real-time inverse kinematics," *International Journal of Control, Automation and Systems*, vol. 18, no. 8, pp. 2095–2107, Aug. 2020, doi: 10.1007/s12555-019-0076-7.

[7]   J. Podobnik, M. Munih, and M. Mihelj, "Magneto-inertial data sensory fusion based on Jacobian weighted-left-pseudoinverse," in *Advances in Robot Kinematics 2020*, Springer International Publishing, 2021, pp. 174–181.

[8]   P. Yotchon and Y. Jewajinda, "Combining a differential evolution algorithm with cyclic coordinate descent for inverse kinematics of manipulator robot," in *2021 3rd International Conference on Electronics Representation and Algorithm (ICERA)*, Jul. 2021, pp. 35–40, doi: 10.1109/ICERA53111.2021.9538798.

[9]   H. M. Tuan, F. Sanfilippo, and N. V. Hao, "Modelling and control of a 2-DOF robot arm with elastic joints for safe human-robot interaction," *Frontiers in Robotics and AI*, vol. 8, Aug. 2021, doi: 10.3389/frobt.2021.679304.

[10] X. Wang, X. Liu, L. Chen, and H. Hu, "Deep-learning damped least squares method for inverse kinematics of redundant robots," *Measurement*, vol. 171, Feb. 2021, doi: 10.1016/j.measurement.2020.108821.

[11] N. V. Toan and P. B. Khoi, "A SVD-least-square algorithm for manipulator kinematic calibration based on the product of exponentials formula," *Journal of Mechanical Science and Technology*, vol. 32, no. 11, pp. 5401–5409, Nov. 2018, doi: 10.1007/s12206-018-1038-3.

[12] P. Sutyasadi and M. B. Wicaksono, "Robotic arm joint position control using iterative learning and mixed sensitivity H∞ robust controller," *Bulletin of Electrical Engineering and Informatics (BEEI)*, vol. 10, no. 4, pp. 1864–1873, Aug. 2021, doi: 10.11591/eei.v10i4.3059.

[13] N. H. Quang, N. Van Quyen, and N. N. Hien, "Radial basis function neural network control for parallel spatial robot," *Telecommunication Computing Electronics and Control (TELKOMNIKA)*, vol. 18, no. 6, Dec. 2020, doi: 10.12928/telkomnika.v18i6.14913.

[14] Y. I. Al Mashhadany, "Virtual reality trajectory of modified PUMA 560 by hybrid intelligent controller," *Bulletin of Electrical Engineering and Informatics*, vol. 9, no. 6, pp. 2261–2269, Dec. 2020, doi: 10.11591/eei.v9i6.2579.

[15] T. Dewi, P. Risma, and Y. Oktarina, "Fruit sorting robot based on color and size for an agricultural product packaging system," *Bulletin of Electrical Engineering and Informatics*, vol. 9, no. 4, pp. 1438–1445, Aug. 2020, doi: 10.11591/eei.v9i4.2353.

[16] Diestra AI, "xArm Lewansoul ROS documentation," 2021. Accessed: Nov 20, 2021. [Online]. Available: https://xarm-lewansoul-ros.readthedocs.io/_/downloads/en/latest/pdf/.

[17] D. Kusmenko and K. Schmidt, "Development of an analytical inverse kinematics for a 5 DOF manipulator," in *2020 21st International Conference on Research and Education in Mechatronics (REM)*, Dec. 2020, pp. 1–5, doi: 10.1109/REM49740.2020.9313880.

[18] W. S. Pambudi, E. Alfianto, A. Rachman, and D. P. Hapsari, "Simulation design of trajectory planning robot manipulator," *Bulletin of Electrical Engineering and Informatics*, vol. 8, no. 1, pp. 196–205, Mar. 2019, doi: 10.11591/eei.v8i1.1179.

[19] F. Maric, M. Giamou, A. W. Hall, S. Khoubyarian, I. Petrovic, and J. Kelly, "Riemannian optimization for distance-geometric inverse kinematics," *IEEE Transactions on Robotics*, vol. 38, no. 3, pp. 1703–1722, Jun. 2022, doi: 10.1109/TRO.2021.3123841.

[20] P. Beeson and B. Ames, "TRAC-IK: An open-source library for improved solving of generic inverse kinematics," in *2015 IEEE-RAS 15th International Conference on Humanoid Robots (Humanoids)*, Nov. 2015, pp. 928–935, doi: 10.1109/HUMANOIDS.2015.7363472.

[21] H. F. Durrant-Whyte, "Uncertain geometry in robotics," *IEEE Journal on Robotics and Automation*, vol. 4, no. 1, pp. 23–31, 1988, doi: 10.1109/56.768.

[22] A. Steinhauser and J. Swevers, "An efficient iterative learning approach to time-optimal path tracking for industrial robots," *IEEE Transactions on Industrial Informatics*, vol. 14, no. 11, pp. 5200–5207, Nov. 2018, doi: 10.1109/TII.2018.2851963.

[23] L. E. J. Alkurawy, "Recursive least square and control for PUMA robotics," *Indonesian Journal of Electrical Engineering and Computer Science (IJEECS)*, vol. 21, no. 2, pp. 1238–1246, Feb. 2021, doi: 10.11591/ijeecs.v21.i2.pp1238-1246.

[24] B. Koyuncu and M. Güzel, "Software development for the kinematic analysis of a Lynx 6 robot arm," *International Journal of Computer and Information Engineering*, vol. 1, no. 6, pp. 1575–1580, 2007.

[25] A. Mathur, C. Bansal, S. Chauhan, and O. Yadav, "A review of pick and place operation using computer vision and ROS," in *Computational and Experimental Methods in Mechanical Engineering*, Springer Singapore, 2022, pp. 411–418.

[26] G. Xu and Y. Yan, "A scene feature based eye-in-hand calibration method for industrial robot," in *Mechatronics and Machine Vision in Practice 4*, Cham: Springer International Publishing, 2021, pp. 179–191.

[27] M. Ahmad, I. Ahmed, and A. Adnan, "Overhead view person detection using YOLO," in *2019 IEEE 10th Annual Ubiquitous Computing, Electronics and Mobile Communication Conference (UEMCON)*, Oct. 2019, pp. 627–633, doi: 10.1109/UEMCON47517.2019.8992980.

[28] O. Martínez and R. Campa, "Comparing methods using homogeneous transformation matrices for kinematics modeling of robot manipulators," in *Multibody Mechatronic Systems*, Springer International Publishing, 2021, pp. 110–118.

BIOGRAPHIES OF AUTHORS

Abhilasha Singh received the B.E. degree in Electrical and Electronics engineering from Jerusalem College of Engineering, Chennai, India in 2013 and the M.E. degree in Instrumentation engineering from MIT, Anna University, Chennai, India, in 2017. She is currently pursuing a Ph.D. degree in Electrical and Electronics Engineering at Birla Institute of Technology and Science Pilani, Dubai Campus since 2018. Her current research area focuses on robotics, computer vision, and intelligent control techniques. She can be contacted at p20180906@dubai.bits-pilani.ac.in.

Kalaichelvi Venkatesan is an associate professor in the Department of Electrical and Electronics Engineering at BITS Pilani, Dubai Campus. She is working with Bits Pilani, Dubai Campus since 2008 and she is having 29 years of teaching experience. She has her research work published in refereed international journals and many international conferences. She has also reviewed many papers in international journals and conferences. Her research area of expertise includes process control, neural networks, fuzzy logic, computer vision, and control systems. She is currently guiding students in the area of intelligent control techniques applied to robotics and mechatronics. She can be contacted at kalaichelvi@dubai.bits-pilani.ac.in.

Yuvalakshmi Nagarasan is a final year B.E. Electrical and Electronics Engineering student at BITS Pilani-Dubai Campus. She is well-versed in power systems, design, and development in the fundamentals of electrical engineering and automation. She is equipped with the knowledge of several software required for robotic manipulation such as Python and MATLAB. Her research interests include power systems, sustainable energy, and robotics. She can be contacted at f20180047@dubai.bits-pilani.ac.in.

Karthikeyan Ramanujam is a professor in the Department of Mechanical Engineering at Bits Pilani, Dubai Campus. He is working with BITS Pilani, Dubai Campus since 2007 and is having 30 years of teaching experience. He has also guided five Ph.D. scholars. He has published over 75 papers in international journals and conferences. He has also reviewed many papers in international journals and conferences. His research area of expertise includes material processing, manufacturing engineering, mechatronics, and robotics. He can be contacted at rkarthikeyan@dubai.bits-pilani.ac.in.

Kumar Karuppusamy is a professor in the Department of General Science at BITS Pilani, Dubai Campus. He is working with Bits Pilani, Dubai Campus since 2004 and is having 33 years of teaching experience. His research area of expertise includes nonlinear dynamics, heat transfer and wave theory. He can be contacted at kumar@dubai.bits-pilani.ac.in.